First publ. in: Physical Review Letters 105 (2010), 066402
DOI 10.1103/PhysRevLett.105.066402

Disentanglement of the Electronic and Lattice Parts of the Order Parameter in a 1D Charge Density Wave System Probed by Femtosecond Spectroscopy

H. Schäfer,[1] V. V. Kabanov,[2,3] M. Beyer,[1] K. Biljakovic,[4] and J. Demsar[1,2,3]
[1]*Physics Department and Center of Applied Photonics, Universität Konstanz, D-78457, Germany*
[2]*Zukunftskolleg, Universität Konstanz, D-78457, Germany*
[3]*Complex Matter Department, Jozef Stefan Institute, SI-1000, Ljubljana, Slovenia*
[4]*Institute of Physics, Hr-10000 Zagreb, Croatia*

We report on the high resolution studies of the temperature (T) dependence of the $q = 0$ phonon spectrum in the quasi-one-dimensional charge density wave (CDW) compound $K_{0.3}MoO_3$ utilizing time-resolved optical spectroscopy. Numerous modes that appear below T_c show pronounced T dependences of their amplitudes, frequencies, and dampings. Utilizing the time-dependent Ginzburg-Landau theory we show that these modes result from linear coupling of the electronic part of the order parameter to the $2k_F$ phonons, while the (electronic) CDW amplitude mode is overdamped.

DOI: 10.1103/PhysRevLett.105.066402 PACS numbers: 71.45.Lr, 72.15.Nj, 78.47.J−

Femtosecond optical spectroscopy is becoming an important tool for investigation of the so-called strongly correlated systems due to its intrinsic ability to determine the interaction strengths between various degrees of freedom which lead to fascinating phenomena like superconductivity or giant magnetoresistance. Low dimensional charge density wave (CDW) systems, with their inherently multicomponent order parameter (modulation of carrier density is accompanied by the modulation of the underlying lattice) present no exception. In the past decade or so various one- and two-dimensional CDWs have been studied by time-resolved optical [1–6] as well as photoemission [7,8] techniques. The initial focus of research was in identifying various components in the observed photoinduced transients with the corresponding ones obtained by standard time-averaging spectroscopic techniques, as well as in coherent control of the collective modes [9]. Recently it was shown that photoexcitation with an intense optical pulse can nonthermally drive the phase transition from the low temperature CDW state to a metastable state, characterized by a suppressed carrier modulation with the lattice remaining nearly frozen [6]. This observation has an important implication for the understanding of ultrafast relaxation processes in this class of materials, and, as we will show, for the general understanding of the cooperative phenomena leading to the appearance of the CDW state and the nature of their collective excitations.

In this Letter we present high resolution studies of T-dependent time-resolved reflectivity dynamics in a prototype quasi-1D CDW material $K_{0.3}MoO_3$. The high sensitivity achieved in this experiment enabled us to measure the T evolution of the low frequency phonons with unprecedented resolution. We were able to show that not only the 1.68 THz (57 cm^{-1}) mode, that is commonly assigned to the collective amplitude mode (AM) of the CDW, shows softening upon increasing T towards $T_c = 183$ K, the phase transition to the normal metallic state. Qualitatively the same softening is observed also for a number of phonon modes that appear below T_c. The frequencies of these modes correspond well to the phonon frequencies at the $2k_F$ modulation vector as observed by neutron experiments [10,11], and are shown to result from the linear coupling of the electronic part of the order parameter (EOP), Δ, to $2k_F$ phonons. Utilizing the time-dependent Ginzburg-Landau (TDGL) model we were able to account for the T dependence of mode frequencies, dampings, and their amplitudes. Surprisingly, the coupling strengths to the EOP of all the modes that show softening is nearly the same. The analysis suggests that in $K_{0.3}MoO_3$ the nonadiabatic regime is realized, where electronic modulation does not adiabatically follow the lattice. The amplitude mode of the EOP, describing the initial recovery of the electronic density modulation, is shown to be an overdamped mode whose damping time diverges as $|\Delta|^{-2}$.

We studied the T dependence of the PI reflectivity dynamics in single crystals of blue bronze $K_{0.3}MoO_3$ using an optical pump-probe technique. A commercial Ti:sapphire amplifier producing 40 fs laser pulses at $\lambda = 800$ nm (photon energy of 1.55 eV) at a 250 kHz repetition rate was used as a source of both pump and probe pulse trains. The probe laser beam ($\vec{E}$) was polarized either along the chain direction ($\vec{b}$) or along the perpendicular (102) direction [12], while the pump beam was always polarized at an angle of 45° with respect to the probe polarization. The induced changes in reflectivity (R) were recorded utilizing a fast-scan technique, enabling high signal-to-noise levels. The excitation fluence was kept at 30 $\mu J/cm^2$, well below the nonlinear regime [6], yet resulting in a large photoinduced reflectivity change, enabling the dynamic range of the signal of $\approx 10^4$.

Figure 1(a) presents the induced reflectivity transients taken at 10 K with $\vec{E} \parallel \vec{b}$ (data for $\vec{E} \perp \vec{b}$ are shown in

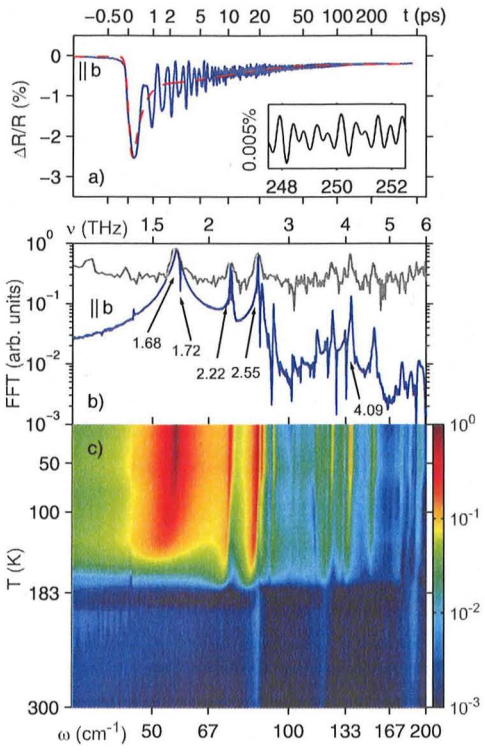

FIG. 1 (color online). (a) Transient change in reflectivity of $K_{0.3}MoO_3$ with $\vec{E} \parallel \vec{b}$ at 10 K following photoexcitation with a 40 fs laser pulse. Dashed line is the fitted electronic transient. Inset: blowup of the response near 250 ps. (b) The FFT spectrum (amplitude) of the coherent parts of the signals, compared to the recent Raman data (gray) from Ref. [14]. (c) The T dependence of the corresponding FFT spectrum in the range between 1–6 THz.

[13]). The transient can be decomposed into an electronic part, which shows a biexponential decay with time scales $\tau_1 \approx 0.2$ ps and $\tau_2 \approx 5$ ps [6], and a coherent part whose Fourier transform, obtained by the fast Fourier transform (FFT) analysis, is shown in panel (b). The FFT shows numerous frequency components which can be attributed to the coherently excited phonon modes [1,4,6]. Most of the observed modes are seen also in Raman [14]; however, the far superior dynamic range and frequency resolution (≈ 0.1 cm^{-1}) of the data obtained by the time-resolved technique enables detailed study of their T dependence.

Figure 1(c) shows the T dependence of the corresponding FFT spectrum. Most of the modes are seen only below T_c implying that these modes result from the symmetry breaking in the CDW phase. Noteworthy, not only the 1.68 THz mode, which is commonly referred to as the amplitude mode of the CDW, but also numerous higher frequency modes show comparable softening as $T \to T_c$. To analyze the T dependence of the modes we fit the FFT data with a sum of damped oscillators. To do so, we first fit the mode that has the strongest amplitude, subtract the resulting fit from the raw data, and perform the same routine on the residual signal to extract the data on the next most intense mode. The T dependence of the seven lowest frequency modes is shown in Fig. 2(b). We see that three modes in this frequency range show pronounced softening as $T \to T_c$, while the frequencies of four very narrow modes at 1.36, 1.72, 2.23, and 2.58 THz remain constant within the experimental accuracy. The frequencies of the most intense modes at 1.68, 2.22, and 2.55 THz, match well with the modes at $2k_F$ as seen in neutron experiments [10,11]—see Fig. 2(a). These observations suggest that these modes, observed in time-resolved experiments as well as in Raman (both probing at $q = 0$), originate from some type of "zone folding" mechanism, as argued earlier [4,6,14]. As we show below, this "folding" can be naturally explained by considering linear coupling of the EOP with the $2k_F$ phonons.

The CDW transition in $K_{0.3}MoO_3$ (space group $C2/m$), is characterized by the modulation wave vector (1, η, -0.5) which corresponds to the vector k_3 of the Brillouin zone (BZ) in Kovalev's notation [15]. This vector is the non-Lifshitz point of the BZ and describes the appearance of an incommensurate structural and electron density modulation; the modulation is incommensurate down to the lowest T with η approaching 0.75 [12]. Vector k_3 belongs to the two-arms star of the wave vector with prongs transforming one to another via inversion ($K_{0.3}MoO_3$ retains the inversion symmetry in the CDW phase [16]). Therefore, the small group has two elements and two irreducible representations and the CDW phase transition is characterized by the two component order parameter. The order parameter can be represented by a complex number $\Delta = \Delta_1 + i\Delta_2$, where Δ_1 and Δ_2 are the real

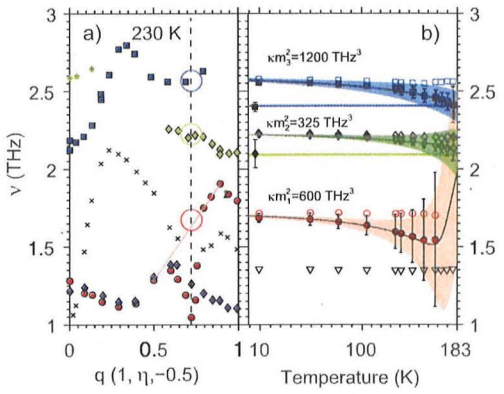

FIG. 2 (color online). (a) Phonon dispersion in (1, η, -0.5) direction at 230 K—reproduced from Ref. [10]. The dashed line corresponds to the CDW modulation wave vector, while the solid line is the expected dispersion of the LA mode at $T \gg T_c$. (b) The T dependence of selected phonon modes: measured ν and $\Gamma/2\pi$ (solid symbols and bars) fit with the model (solid lines and shaded areas)—see also [13]. The values of κm_i^2 (in units THz^3) obtained from the fit are shown. The frequencies (dampings) of the infrared modes at 6 K from Ref. [16] are shown by solid black symbols.

and imaginary parts, and $|\Delta| = (\Delta_1^2 + \Delta_2^2)^{1/2}$. Since below T_c different modes appear at $q = 0$ we include in the thermodynamic potential the modes coupled linearly to the order parameter. Such a procedure does not make sense if one considers the thermodynamical properties of the system only. When discussing the dynamical properties of the system, such as the normal modes, these terms have to be included, as discussed in Ref. [17]. Therefore we define $\Delta_{1,2}$ as a purely EOP associated with the $2k_F$ carrier density modulation. It is in general linearly coupled with any lattice displacement at $2k_F$ which transforms as the τ_1 representation of the small group. Deformations belonging to 4, 6, $8k_F$ may be coupled only to the higher orders of the EOP and are therefore not included. In the strictly incommensurate case, when the phase transition is associated with a non-Lifshitz wave vector, the higher order invariants are also absent (the thermodynamic potential does not depend on the phase of the order parameter [18,19]). The resulting thermodynamic potential can be written as

$$\phi = \phi_0 + \frac{1}{2}\alpha(T - T_{c0})(\Delta_1^2 + \Delta_2^2) + \frac{1}{4}\beta(\Delta_1^2 + \Delta_2^2)^2 + \frac{\Omega_0^2}{2}(\xi_1^2 + \xi_2^2) - m(\Delta_1\xi_1 + \Delta_2\xi_2). \quad (1)$$

Here ϕ_0 corresponds to the high-T phase, α, $\beta > 0$ are the standard GL constants, $\xi_{1,2}$ are generalized coordinates of displacements which transform as τ_1 representations of the small group. Ω_0 is the frequency of the vibrational mode at $T \gg T_{c0}$, where T_{c0} is the bare critical temperature (in the absence of coupling to the lattice) and m describes the strength of the coupling between the mode and the EOP. Here we assume that the effective mass of the mode is equal to 1. To minimize ϕ we choose the following (equilibrium) solution: $\xi_2^{(0)} = \Delta_2^{(0)} = 0$, $\Delta_1^{(0)} = \sqrt{\alpha(T_c - T)/\beta}$ and $\xi_1^{(0)} = \frac{m\Delta_1^{(0)}}{\Omega_0^2}$. The observable T_c is renormalized due to the coupling with the displacement and is given by $T_c = T_{c0} + \frac{m^2}{\alpha\Omega_0^2}$. For the illustrative purpose we include only one mode coupled to the EOP, but the result can be generalized to all same symmetry modes at $2k_F$ that are coupled to $\Delta_{1,2}$ linearly [13].

Let us now consider the equations of motion of the EOP and the phonon mode assuming small fluctuations near their equilibrium positions, i.e., $\Delta_{1,2}(t) = \Delta_{1,2}^{(0)} + x_{1,2}(t)$ and $\xi_{1,2}(t) = \xi_{1,2}^{(0)} + y_{1,2}(t)$. We can assume the electronic mode to be overdamped, since the frequency of the bare mode $\omega = \sqrt{2}|\Delta|$ lies above the gap for single particle excitations, as in the case of a spin density wave [12]. The equations for the real parts of the order parameter (x_1, y_1), describing the overdamped amplitude mode of the electronic channel and the Raman active lattice vibration, respectively, are

$$\begin{aligned} \dot{x}_1 &= -2\kappa\alpha\left(T_c - T + \frac{m^2}{2\alpha\Omega_0^2}\right)x_1 - \kappa m y_1 \\ \ddot{y}_1 &= -\Omega_0^2 y_1 - m x_1, \end{aligned} \quad (2)$$

κ^{-1} being the analog of the friction coefficient. Similar analysis for the infrared modes [16,20] is presented in [13]. The general solution of Eqs. (2) can be found in the form of $x_1 = a_1 \exp(\lambda_1 t)$ and $y_1 = b_1 \exp(\lambda_1 t)$ resulting in a cubic equation for λ_1:

$$\lambda_1^3 + 2\kappa\alpha\left(T_c - T + \frac{m^2}{2\alpha\Omega_0^2}\right)\lambda_1^2 + \Omega_0^2\lambda_1 + 2\kappa\alpha\Omega_0^2(T_c - T) = 0. \quad (3)$$

At $T = T_c$ it follows that $\lambda_1^{(1)} = 0$, indicating that the relaxation time for the EOP diverges, while $\lambda_1^{(2,3)} = \pm i\Omega_0\sqrt{1 - (\kappa m^2/2\Omega_0^3)^2} - \frac{\kappa m^2}{2\Omega_0^2}$. The mode frequency $\Omega(2\pi\nu) = \mathrm{Im}(\lambda_1)$ and damping $\Gamma = \mathrm{Re}(\lambda_1)$ at $T = T_c$ exactly correspond to the values of the matching infrared mode [13]. Indeed, for both 2.22 and 2.55 THz modes, we find that the mode frequencies near T_c match well the frequencies of the infrared modes, discussed in Ref. [16] using a similar scenario [16,20].

The above model describes both adiabatic and nonadiabatic limits. In the adiabatic limit, when $\Gamma_{EOP} \gg \Omega_0$, the phonon mode is a true soft mode with $\Omega_0 \rightarrow 0$ at T_c—see [13]. In the intermediate (nonadiabatic) case, however, Ω shows softening only until $\Gamma_{EOP} \approx \Omega_0$, while in the vicinity of the phase transition Ω can also increase. The solutions of Eq. (3) for the intermediate case are shown in insert to Fig. 3(a). Indeed, in the entire class of materials $\Gamma_{EOP} \approx \Omega_0$, with damping of the fast electronic component showing critical slowing down towards T_c [1,3,5]—see Fig. 3(a). This suggests, that the fast electronic decay process can be identified as the overdamped mode of the EOP.

Using this simple model we were able to fit the T dependence of Ω and Γ for the three most intense phonon modes—see Fig. 2(b). The agreement between the measured frequencies (symbols) and Ω's from the model (solid lines) is nearly perfect. A very good agreement is also found between the measured (error bars) and model (shaded areas) damping constants. Given the simplicity of the model, assuming a GL T dependence of $|\Delta|^2$ over the entire T range, the fact that other processes (e.g., dephasing) can also contribute to the damping, the agreement is excellent. It is noteworthy that the coupling strengths m_i between the EOP and the three most intense phonons [see Eqs. (1)–(3)], obtained by fitting to the model, are nearly identical—see Fig. 2(b).

Figure 3(b) shows the T dependence of mode amplitudes, normalized to their low temperature value. All modes that show pronounced softening near T_c show very similar T dependence of amplitude, which can be well explained within our model. Assuming that the order

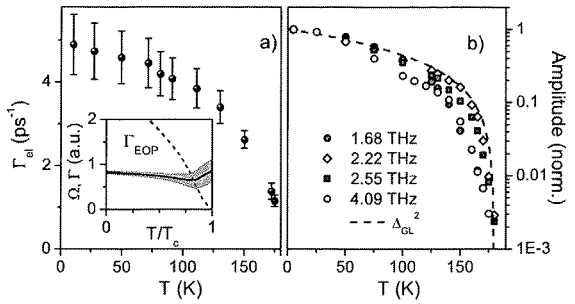

FIG. 3 (color online). (a) The measured T dependence of the fast electronic damping showing critical slowing down at T_c. The inset shows the model simulation with one mode linearly coupled to the EOP, where the solid line (shaded area) represent the phonon mode frequency (damping), while the dashed line represents the damping of the overdamped EOP. (b) The T dependence of normalized amplitudes of modes that show softening. It follows well the expected $|\Delta|^2$ T dependence (dashed line).

parameter is small we can expand the dielectric constant near the CDW phase transition in powers of the order parameter $\Delta_{1,2}$ and variables $\xi_{1,2}$ [21]:

$$\epsilon(k=0) = \epsilon_0 + c_1(\Delta_1^2 + \Delta_2^2) + c_2(\Delta_1\xi_1 + \Delta_2\xi_2) + \ldots . \quad (4)$$

Here ϵ_0 is the dielectric constant of the high-T symmetric phase, and c_1 and c_2 are real constants (linear terms in the expansion are not allowed by symmetry). It follows that the induced change in the displacement ($\xi_{1,2}$) should result in a change in ϵ (or R) that is proportional to $\Delta_{1,2}$. However, since the change in the displacement is itself proportional to the EOP, the mode amplitude—as determined by the time-resolved experiment—should follow the $|\Delta|^2$ T dependence. The data are indeed well fit to the GL T dependence of $|\Delta|^2_{GL} \propto (T_c - T)/T$. Amplitudes of the weak satellite modes, which show nearly no T dependence of frequency, are, however, found to show a substantially faster decrease with T [13]. This suggests that the satellite modes are either $q = 0$ modes, which are amplified below T_c due to coupling to the neighboring "folded" modes (like 2.23 and 2.58 THz modes), or are the result of a higher order coupling to the EOP (1.72 and 1.36 THz modes) [13].

In conclusion, high resolution T dependence studies of photoinduced reflectivity changes in the quasi-1D CDW compound $K_{0.3}MoO_3$ enabled us to track the T dependence of the coherently generated phonon modes with unprecedented sensitivity. Numerous modes that appear below T_c, and show comparable softening as T_c is approached, are observed. By applying TDGL analysis we were able to show that these modes are a result of the linear coupling of the EOP to the $2k_F$ phonons where the EOP does not adiabatically follow the lattice modulation. This interpretation presents an alternative to the fluctuation scenario [10,22], answering the long standing question why no phonon shows full softening near T_c in this class of materials. The fact that a fast electronic dynamics, whose decay time diverges near T_c, is observed in many CDW compounds [1,3,5] lead us to identify this mode as the overdamped (electronic) amplitude mode. The disentanglement of the electronic and lattice parts of the order parameter on the very short time scale, demonstrated here for the CDW systems, could be, however, operational in a broader class of materials undergoing structural phase transitions.

We wish to acknowledge Stefan Eggert for his help with various aspects of data acquisition, D. Sagar for providing us the low temperature Raman data, and valuable discussions with V. Pomjakushin, T. Dekorsy, J. P. Pouget, J. E. Lorenzo, L. Degiorgi, and P. Monceau. The work was supported by the Sofja-Kovalevskaja Grant from the Alexander von Humboldt Foundation, Zukunftskolleg and CAP at the University of Konstanz.

[1] J. Demsar, K. Biljakovic, and D. Mihailovic, Phys. Rev. Lett. **83**, 800 (1999).
[2] J. Demsar *et al.*, Phys. Rev. B **66**, 041101 (2002).
[3] K. Shimatake, Y. Toda, and S. Tanda, Phys. Rev. B **75**, 115120 (2007).
[4] D. M. Sagar *et al.*, J. Phys. Condens. Matter **19**, 346208 (2007).
[5] R. V. Yusupov *et al.*, Phys. Rev. Lett. **101**, 246402 (2008).
[6] A. Tomeljak *et al.*, Phys. Rev. Lett. **102**, 066404 (2009).
[7] L. Perfetti *et al.*, Phys. Rev. Lett. **97**, 067402 (2006); L. Perfetti *et al.*, New J. Phys. **10**, 053019 (2008).
[8] F. Schmitt *et al.*, Science **321**, 1649 (2008).
[9] D. Mihailovic *et al.*, Appl. Phys. Lett. **80**, 871 (2002); T. Onozaki, Y. Toda, S. Tanda, and R. Morita, Jpn. J. Appl. Phys. **46**, 870 (2007).
[10] J. P. Pouget *et al.*, Phys. Rev. B **43**, 8421 (1991).
[11] C. Escribe-Filippini, J. P. Pouget, R. Currat, B. Hennion, and J. Marcus, in *Lecture Notes in Physics* (Springer-Verlag, Heidelberg, 1985), Vol. 217, pp. 71–75.
[12] G. Grüner, *Density Waves in Solids* (Addison-Wesley, Reading, MA, 1994).
[13] See supplementary material at http://link.aps.org/supplemental/10.1103/PhysRevLett.105.066402.
[14] D. M. Sagar *et al.*, New J. Phys. **10**, 023043 (2008).
[15] O. V. Kovalev, *Irreducible Representations of the Space Groups* (Gordon and Breach, New York, 1965).
[16] L. Degiorgi, B. Alavi, G. Mihály, and G. Grüner, Phys. Rev. B **44**, 7808 (1991).
[17] D. G. Sannikov, Phys. Solid State **50**, 746 (2008).
[18] Y. A. Izyumov and V. N. Syromyatnikov, *Fazovye Perekhody I Simmetriya Kristallov* (Nauka, Moskow, 1984) (in Russian).
[19] J. Ollivier *et al.*, Phys. Rev. Lett. **81**, 3667 (1998).
[20] M. J. Rice, Phys. Rev. Lett. **37**, 36 (1976).
[21] V. L. Ginzburg, Sov. Phys. Usp. **5**, 649 (1963).
[22] E. Tutis and S. Barisic, Phys. Rev. B **43**, 8431 (1991).